

# Improved StyleGAN Embedding: Where are the Good Latents?

Peihao Zhu<sup>1</sup> Rameen Abdal<sup>1</sup> Yipeng Qin<sup>2</sup> Peter Wonka<sup>1</sup>

<sup>1</sup>KAUST <sup>2</sup>Cardiff University

{peihao.zhu, rameen.abdal}@kaust.edu.sa qiny16@cardiff.ac.uk pwonka@gmail.com

## Abstract

*StyleGAN is able to produce photorealistic images almost indistinguishable from real ones. Embedding images into the StyleGAN latent space is not a trivial task due to the reconstruction quality and editing quality trade-off. In this paper, we first introduce a new normalized space to analyze the diversity and the quality of the reconstructed latent codes. This space can help answer the question of where good latent codes are located in latent space. Second, we propose a framework to analyze the quality of different embedding algorithms. Third, we propose an improved embedding algorithm based on our analysis. We compare our results with the current state-of-the-art methods and achieve a better trade-off between reconstruction quality and editing quality.*

## 1. Introduction

GAN inversion (embedding) refers to the task of computing a latent code for a given input image. The goal of the embedding is typically to perform some subsequent image processing tasks such as image interpolation or semantic image editing. Due to the high visual quality of generated images and comparatively lightweight architecture, most recent papers build on StyleGAN [15] and StyleGAN2 [16, 14] for their embedding algorithms. The resulting embeddings differ in two main aspects: the reconstruction quality and the editing quality. The reconstruction quality considers how similar an embedded image is to the input image and how realistic the embedded image is. The editing quality describes the visual quality of images after editing operations, such as image interpolation, or pose and lighting changes for faces.

In this paper, we set out to provide some analysis of existing embedding methods. We propose a suitable space, called  $P$ -norm space to perform the analysis. In  $P$ -norm space, the distribution of StyleGAN latent codes has a surprisingly simple structure. This enables an explanation of where good latent codes can be found. A major insight of

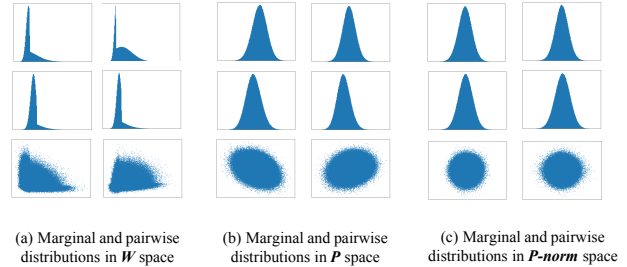


Figure 1: Marginal and pair-wise distributions of different spaces in StyleGAN. First and second rows: the marginal distribution of a randomly picked latent variable. Third row: the pairwise joint distribution of two randomly picked latent variables.

the analysis is that the quality of a latent code is closely related to the distance from the center of  $P$ -norm space. Unfortunately, reconstruction quality favors latent codes that are far from the center, but editing quality favors latent codes close to the center. This requires a trade-off between reconstruction quality and editing quality. Investigating the individual dimensions of latent codes in  $P$ -norm space already gives a strong understanding of the trade-offs made by current methods. For example, the step size and the learning rate in Image2StyleGAN [1] controls the trade-off between reconstruction quality and editing quality. By contrast, current embedding networks, e.g. [17, 16, 21], always create embeddings close to the center and strongly favor editing quality over reconstruction quality. As a next step, we will propose a framework for evaluating embedding algorithms. The framework consists of a sequence of tests to evaluate the reconstruction quality and editing quality of embedded images. Finally, we propose an improved embedding algorithm that clearly outperform all existing methods by forcing the embeddings to stay closer to the center of the  $P$ -norm space. Our main contributions are:

- the introduction of  $P$ -norm space for analyzing and regularizing StyleGAN embeddings.

- a framework to compare different embedding algorithms and a corresponding analysis demonstrating the advantages and disadvantages of different methods.
- a new embedding algorithm that provides the best trade-off between reconstruction and editing quality.

## 2. Related Work

The seminal paper by Goodfellow et al. [8] started an avalanche of GAN papers that together lead to impressive improvements over the last years [20, 4, 13, 19, 15, 16, 14]. Similar to most other work in GAN image embedding, we build on StyleGAN [16, 15, 14] due to its exceptional visual quality and comparatively lightweight architecture.

Since the recent inception of Image2StyleGAN (I2S) [1] which first proposed a feasible method to embed a given image into the  $W^+$  latent space of the StyleGAN generator, there have been many works trying to improve upon the initial idea.

Most of the existing methods have the same goal: finding a balance between the reconstruction quality and the editing quality. For example, I2S++ [2] improved the reconstruction quality of I2S by incorporating a noise optimization step to restore the high-frequency details in the input image. Similarly, StyleGAN2 [16] uses an additive ramped-down noise to help the latent space exploration. These two methods lead to different trade-offs: I2S++ embeds images into the  $W^+$  space that sacrifices a bit of editing quality to achieve better reconstruction quality; while on the contrary, the StyleGAN2 embeds images in the  $W$  space that enables better editing but at the cost of worse reconstruction. Following a different approach, PIE [24] first embeds an image into the  $W$  space for better editing quality and then improves the reconstruction quality by optimizing the latent obtained in the  $W^+$  space. Such a two-stage encoding process is also employed by several concurrent works based on encoder networks [6, 29, 10, 5], which to our knowledge first appears in iGAN [30]. In their methods, an initial latent code is first obtained by passing the input image through a pre-trained StyleGAN encoder. Then, the initial latent code is further optimized to improve its reconstruction quality. Using only the encoder network by itself leads to poor reconstruction quality.

Unlike previous methods, PULSE [17] formulated embedding as traversing the manifold consisting of good latents. However, they regularized the latents to be on the surface of a hypersphere that only contains a subset of good latents. As a result, their method usually leads to poorer reconstruction quality. Inspired by PULSE, in this work, we provide a thorough analysis of where the good latents are and how to evaluate an embedding. Based on our analysis, we propose an improved embedding algorithm that outperforms all existing methods.

## 3. Which Space to Use: a Statistical Analysis of Latent Distributions

The goal of this section is to identify a space where the distribution of latent codes has a simple structure. A suitable space will make it easier to reason about good and bad latent codes for the StyleGAN generator [15, 16]. However, the interpretability challenge of deep neural networks makes it difficult to determine which latent space is better. Following the philosophy of *Occam's razor* [7], we conjecture that a good latent space is one in which the latent distribution can be characterized in the simplest possible way. To find such a latent space, we conduct a statistical analysis on the latent distributions in different latent spaces as follows (See Fig. 4).

**$W$  Space:** The  $W$  space proposed in StyleGAN [15] is the most straightforward choice of latent space. Therefore, we start our investigation by sampling 1 million latents in  $W$  space and visually checking the statistics of their marginal distributions. As Fig. 1 (a) shows, the marginal distributions are heavily skewed and do not follow any obvious patterns. Thus, the  $W$  space latent distribution is difficult to characterize and not suitable for the classification of good and bad latents.

**$P$  Space:** To get rid of the skewness of marginal distributions, we transformed the  $W$  space to the  $P$  space [17] by inverting the last Leaky ReLU layer in the StyleGAN mapping network. Similar to those in  $W$  space, we plot the marginal distributions of latents in  $P$  space and observed that they nicely follow a simple Gaussian-like distribution. Although this is a great start, it is unclear how much the latents depend on each other. Therefore, we plot the pairwise joint distribution of latents (See Fig. 1b) and observed that the dimensions are indeed dependent. We make the simplest assumption that the joint distribution of latents is approximately a multi-variate Gaussian distribution. This motivates us to introduce the  $P$ -norm Space in which the latent distribution is easier to characterize.

**$P$ -norm Space:** Our  $P$ -norm space aims to i) eliminate the dependency among latent variables; ii) remove redundancy and only capture the major information of the latent distribution. To fulfill these two aims, we first construct the  $P$ -norm space using the orthonormal basis obtained by applying Principal Component Analysis (PCA) to StyleGAN latents in  $P$  space. Then, we adjust the position and scale of the orthonormal basis to normalize the distribution of each latent variable to be of zero mean and unit variance. As a result, the latent distribution in our  $P$ -norm space will look like a ball that is isotropic in all directions (Fig. 1c).



Figure 2: Editing quality of different embedding methods using the StyleGAN2 generator. Row-wise: **I2S\***: Image2StyleGAN on StyleGAN2; **PUL\***: PULSE on StyleGAN2; **S2E**: StyleGAN2Encoder; **SG2**: StyleGAN2. Column-wise: (I) Reconstruction; (II) Pose edit; (III) Gender edit; (IV) Style mixing; (V)  $W^+$  Space Interpolation (middle point) (VI) Projected  $P$ -norm $^+$  space interpolation (middle point). (a) Input image; (b) Content image in (IV) and the second input image in (V) and (VI).).

To verify the validity of our  $P$ -norm space, we independently sample each dimension in  $P$ -norm space and compare the FID scores we get with those of StyleGAN2 [16].  $P$ -norm space sampling yields an FID of 3.28 compared to an FID of 2.81, justifying the validity of our  $P$ -norm space. Although good for characterization of latent distributions,  $P$ -norm space is too small for image embedding. To this end, we extend it to  $P$ -norm $^+$  space following a standard practice proposed in [1].

**$P$ -norm $^+$  Space:** Similar to the extension from  $W$  space to  $W^+$  space [1], we extend  $P$ -norm space to  $P$ -norm $^+$  space by concatenating 18 different 512-dimensional  $P$ -norm latents. Each of the latents is used to demodulate the corresponding StyleGAN feature maps at different layers. We propose to use  $P$ -norm $^+$  space to analyze and regularize StyleGAN inversion algorithms.

Method	SSIM	RMSE	PSNR	VGG	LPIS
I2S* [1]	<u>0.85</u>	<b>0.07</b>	23.30	<b>0.63</b>	0.20
PUL* [17]	0.83	0.09	21.04	1.10	0.37
S2E [21]	<u>0.85</u>	0.08	21.46	0.99	0.33
SG2 [16]	0.80	0.13	18.73	0.85	0.21
Ours	<b>0.86</b>	<b>0.07</b>	<b>23.80</b>	<u>0.70</u>	<b>0.16</b>

Table 1: Quantitative comparison of reconstruction quality. Our method outperforms current leading methods on similarity metrics SSIM, RMSE, PSNR, VGG [23], and LPIPS [28]. Two best results are underlined; best result is bold.

#### 4. How to Evaluate an Embedding?

The purpose of this section is to introduce a framework to evaluate the quality of an embedding algorithm. We pro-

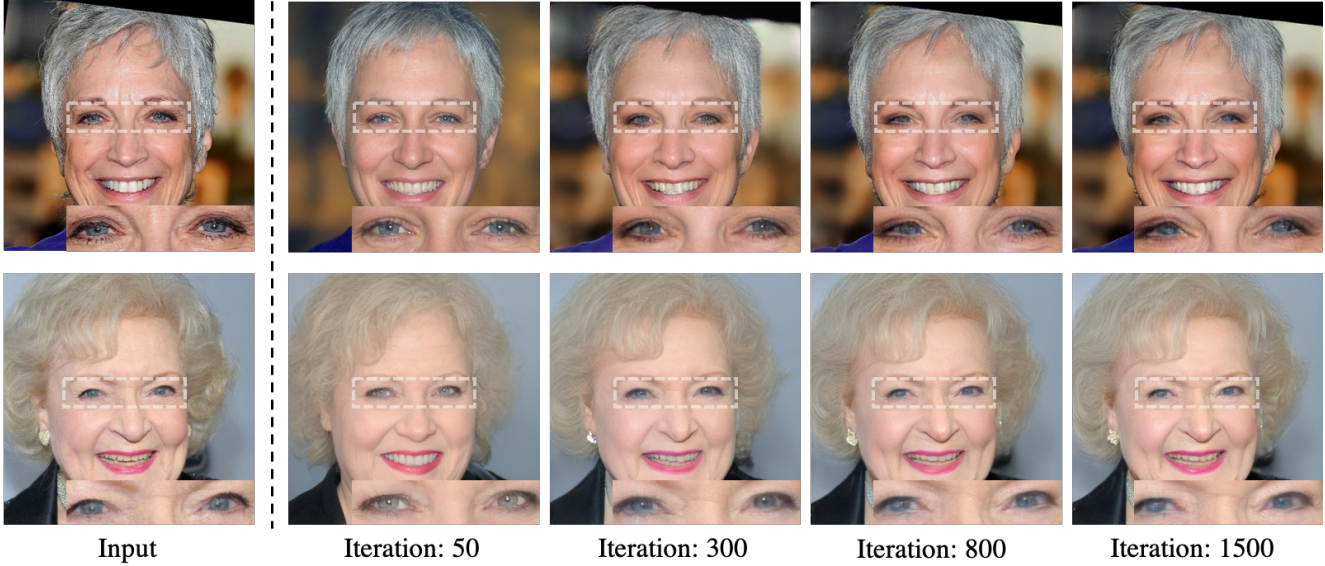


Figure 3: Progression of eye embedding using I2S. Notice that the eyes eventually lose their realism with 800 iterations. The original image is shown to the left.

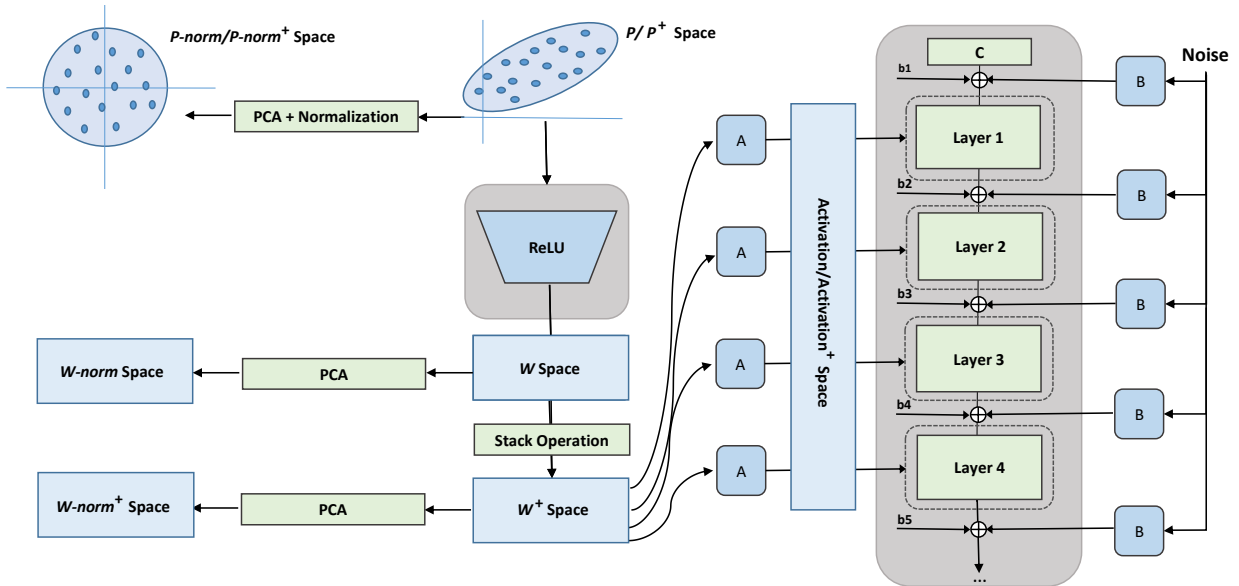


Figure 4: We show five different spaces into which projection of a given image is possible. These are:  $W$  space,  $W^+$  space, Activation space,  $P$  Space and  $P$ -norm space. Notice that translation from  $W$  to  $P$  or  $P$  to  $W$  space goes through an invertible function (Leaky ReLU).

pose a sequence of tests for that purpose.

First, we need to discuss what constitutes a high quality embedding. Then, we describe different methods we compare to and the sequence of tests. While, at this point we did not explain our algorithm yet, we will use the presented framework to explain why our algorithm is preferable to other methods.

#### 4.1. What is a High Quality Embedding?

In general, a good embedding should have the following three properties: i) it should faithfully reconstruct the input image ii) it should be a realistic face image and iii) it should enable realistic editing. We consider i) and ii) to be part of the reconstruction quality and iii) as editing quality. We



Figure 5: Reconstruction quality of different embedding methods using the StyleGAN2 generator.

Method	$W^+$ Space	$P - norm+$ Space
I2S* [1]	54.032	73.844
PUL* [17]	84.404	83.391
S2E [21]	91.439	93.375
SG2 [16]	55.724	61.494
Ours	<b>52.824</b>	<b>51.143</b>

Table 2: Interpolation comparison. We generate 5 samples evenly along the interpolation path and compute the FID with the input images.

Method	PPL		StyleMix	Gender
	Random all	Random	FID	Accuracy
I2S* [1]	66.9	115.0	78.0	0.35
PUL* [17]	26.7	61.2	81.3	0.40
S2E [21]	<b>87.5</b>	<b>155.4</b>	90.8	<b>0.70</b>
SG2 [16]	17.9	36.7	<b>63.6</b>	0.10
Ours	<u>72.4</u>	<u>135.1</u>	<u>72.6</u>	<u>0.50</u>

Table 3: Perceptual Path length: we test two scenarios in which "Random all" considers different values of perturbation for each layer and "Random" is the standard method proposed by StyleGAN2. A lower perceptual path length corresponds to lower editing quality. StyleMix: a lower score indicates better editing quality. Gender: higher accuracy is better.

make a subtle distinction between i) and ii) because some embedding methods have good reconstruction quality when considering traditional similarity metrics, but still have artifacts, e.g. unrealistic eyes and teeth (see Fig. 3).

Method	$-2\sigma$	$-1\sigma$	0	$1\sigma$	$2\sigma$
I2S* [1]	16.27	6.88	-1.14	-9.20	-17.65
PUL* [17]	17.86	8.74	-0.83	-9.57	-17.27
S2E [21]	<b>23.49</b>	9.51	-2.28	-13.76	<b>-26.36</b>
SG2 [16]	11.61	4.96	-1.42	-7.27	-13.25
Ours	<u>20.46</u>	9.04	-1.49	-11.75	<u>-21.86</u>

Table 4: Pose metric for testing the editing quality of the latents. Higher ranges indicate better editing quality.

## 4.2. Competing Methods

We extensively tested many methods that have code available and selected the methods that performed best for a more detailed comparison. We compare our proposed I2S method (Section 5) with the following state-of-the-art methods:

- I2S [1] is the baseline method we would like to improve upon which embeds images into the  $W^+$  space.
- PULSE [17] observed the "soap bubble" effect of high dimensional Gaussian distributions and proposed to embed images onto the surface of a hypersphere in P-space.
- StyleGAN2 [16] embeds images into the W space with the help of noise regularization.
- StyleGAN2Encoder [21] proposed a two-stage embedding method: First, an initial latent code is obtained by passing the input image through a pretrained encoder network. Then, the initial latent code is further optimized in  $W^+$  space using a method similar to I2S.

Note that we reimplemented I2S and PULSE on StyleGAN2 and use good hyperparameter settings for I2S to limit

Method	Reconstruction Metrics				StyleMix	
	SSIM	RMSE	PSNR	VGG	LPIPS	FID
$P\text{-norm}^+$	0.79	0.07	22.53	0.77	0.21	124.29
$P\text{-norm}^+Clip$	0.78	0.08	21.98	0.80	0.23	<b>124.08</b>
$W^+$	<b>0.83</b>	<b>0.06</b>	<b>24.43</b>	<b>0.61</b>	<b>0.14</b>	136.79
$W^+Clip$	0.79	0.07	22.53	0.75	0.21	124.87

Method	Interpolation Metrics	
	$W^+$ Space	$P\text{-norm}$ Space
$P\text{-norm}^+$	123.11	116.05
$P\text{-norm}^+Clip$	119.86	<b>114.05</b>
$W^+$	<b>118.07</b>	223.59
$W^+Clip$	121.83	130.84

Method	Pose Metrics				
	$-2\sigma$	$-1\sigma$	0	$1\sigma$	$2\sigma$
$P\text{-norm}^+$	21.10	11.24	<b>-0.91</b>	<b>-14.55</b>	<b>-25.05</b>
$P\text{-norm}^+Clip$	<b>23.63</b>	<b>12.75</b>	-0.59	-13.86	-24.21
$W^+$	20.68	10.31	-0.56	-10.77	-20.44
$W^+Clip$	23.13	12.15	-0.02	-12.42	-24.01

Table 5: Evaluation of reconstruction and editing quality with clipping regularizer in  $P\text{-norm}^+$  space. The regularizer is applied to both the  $W^+$  code optimized with II2S (see Sec. 5) and the  $P\text{-norm}^+$  code. The FID for the interpolation is achieved by evaluating the middle samples. We achieve a reasonable trade-off, where the editing ability is improved at the small cost of reconstruction quality. The StyleMix and Pose metrics show that the editing quality of the images improve. Please see Fig. 9 for improved realism.

overfitting. We do not compare to the IDInvert method [29] and Multi-code embedding [9] because they only work on the old StyleGAN architecture [15] at a low resolution of  $256 \times 256$ . We also do not use noise embedding as proposed by I2S++ [2] because it is too hard to control with respect to editing quality.

### 4.3. Reconstruction Quality

The measurement of image quality is a fundamental problem in signal processing and communication that has been studied for tens of years. Starting by measuring the absolute differences between images, recent methods gradually turned to measure the perceptual quality that mimics human visual perception. In this work, we measure the reconstruction quality of an embedding both i) absolutely using RMSE, PSNR and ii) perceptually using SSIM, VGG perceptual similarity, LPIPS perceptual similarity and the FID [12] score between the input and embedded image. The results are shown in Table 1. It can be observed that our method has the best reconstruction quality according to all metrics except for VGG. Our method can also be configured to achieve higher reconstruction quality, but that adversely affects editing quality. In Fig. 5, we show the reconstruction quality. Notice that other methods, especially StyleGAN2Encoder, are only similar to the input when viewed at lower resolutions and are less suitable for editing applications.

## 4.4. Editing Quality

Unlike reconstruction, the editing quality of an embedding has not been studied, because competitive editing frameworks just became available very recently [22, 11, 25, 3]. For its simplicity and interpretability, we choose GANSpace [11] as our main evaluation method for editing quality. We propose to test the editing quality using existing editing operations (e.g. pose and gender editing, style mixing), existing metrics (e.g. path length), and latent space exploration (e.g. interpolation). We developed this list as it seems most discriminative for faces, but other edits could also be used. In Fig. 2, we visually compare editing results of different methods. Notice how our method preserves the realism of the images after the edits.

### 4.4.1 Pose Editing

A remarkable property of the GAN latent space is that it contains different views of the same objects (e.g. face poses). We observe that even though current methods evaluate the pose changes based on identity score and FID [3, 25], there is a common pitfall that should be avoided. We observe that some, generally lower quality, embeddings produce smaller degrees of pose change when the same editing operation is applied. Therefore, a method can achieve a better identity and FID score if it does not change the image a lot. To overcome this, we propose to check the editing quality by measuring the degree of pose change using the state-of-the-art classifier Microsoft Face API [18].

For the pose change experiments, we use the right-left

pose edit from GANSpace. Specifically, for a latent code in the GANSpace coordinate system, we can set the coordinate corresponding to pose to five different values:  $-2\sigma$ ,  $-\sigma$ ,  $0$ ,  $\sigma$ , and  $+2\sigma$ , where  $\sigma$  is the eigenvalue for the direction. Table 4 shows the results of pose change edits.

#### 4.4.2 Gender Editing

We also test the gender change direction of GANSpace (See Table 3). We calculate the classification accuracy with the help of Microsoft Face API. Here, we use  $-\sigma$  and  $\sigma$  for the editing strength.

#### 4.4.3 Path Length

The path length metric was introduced by Karras et al. [15] to measure the quality of generated images. This metric is very interesting, but similar to other GAN evaluation metric it has many pitfalls. For example, when editing an image with the same edit strength, we can see the following behavior. Embedded images that are outside the range of the valid space, change a lot less due to an edit and lead to a small path length metric indicating that the embedding is not semantic. Therefore, we can use path length to evaluate the semantic quality of an embedding, but with the catch that a short path length means that the semantic embedding quality is low. Table 3 shows the results on the various methods.

#### 4.4.4 Linear Interpolation

Linear interpolation of latent codes can generate a morph between two embedded images. It is also a powerful tool to determine whether an embedding is semantically meaningful. The nature of the latent space ensures that intermediate images are of high quality as long as the two images being interpolated are of high quality. In other words, we can tell if an embedding is good if the interpolated images between it and a randomly sampled image are of high quality. To this end, we test the interpolation results in both the  $W^+$  and  $P\text{-norm}^+$  space. Table 2 shows the results on various methods. We note that when I2S embedding is projected into the  $P\text{-norm}^+$  space, the interpolation FID becomes worse, again indicating that the distribution is far from the original StyleGAN latent distribution.

#### 4.4.5 Style Mixing

As two sides of the same coin, the results of style mixing and structural edits (*e.g.* pose editing) both reflect how good a latent disentangles the style and contents at different layers of the StyleGAN generator. Thus, it is also worthwhile to check whether an embedding enables high quality style mixing. We take the variables from the first 7 layers from one image and from the remaining 11 layers from another

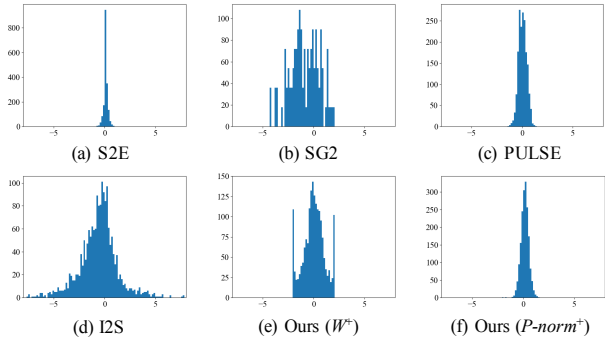


Figure 6: Histograms showing the distribution of latents in the first dimension of the  $P\text{-norm}^+$  Space. Note the strange histogram for SG2. I2S shows a histogram for hyperparameters that overfit.

image and test the FID of the results with the original images. Table 3 shows the result of style mixing on various methods.

#### 4.5. Looking at the “Eyes” and “Mouth”

Several existing evaluations in previous work are flawed, because they overemphasize reconstruction quality in the hyperparameter settings. For example, we could observe that Zhu et al. [29] and Tewari et al. [24] use suboptimal I2S [1] hyperparameter settings for some of the comparisons. One simple test is to check the visual realism of the eyes and teeth during the embedding to observe the transition from reasonable editing quality to overfitting and poor editing quality. In Fig. 3 we show a progression of the embedding process with closeup insets of the eyes of the original I2S algorithm. This simple test is of high practical importance.

#### 4.6. Summary

Based on the reconstruction quality we remark that StyleGAN2 embeddings are almost never recognizable as the same person. PULSE and StyleGAN2Encoder sometimes have a good reconstruction, but sometimes the reconstruction ends up being quite different from the given image. Only Image2StyleGAN and our method have consistent reconstruction quality, with our method being slightly better. In editing quality, StyleGANEncoder and our method have comparable results (in some metrics our method is better in some StyleGANEncoder is better). StyleGANEncoder is actually similar to Image2StyleGAN with a smaller number of iterations. However, it also has some obvious failure cases due to problems with the early stopping heuristic in StyleGANEncoder. Our embedding provides a better trade-off between reconstruction quality and editing quality.

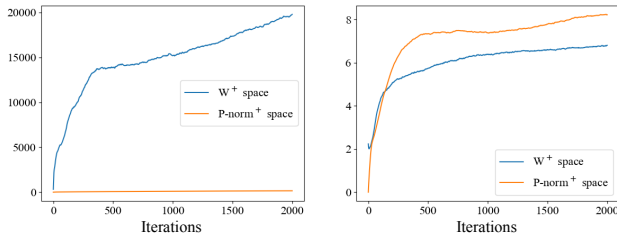


Figure 7: Latents move far from the mean face [15, 1] during the optimization. **Left:** iterations vs Euclidean distances from the mean faces in  $P$ -norm<sup>+</sup> space when optimizing in either  $P$ -norm<sup>+</sup> (orange) or  $W$ <sup>+</sup> space (blue) considering all the dimensions. **Right:** iterations vs Euclidean distances from the mean face in the  $P$ -norm<sup>+</sup> space considering only the first 10 dimensions. Due to the outliers in later dimensions the distances on the left are large when embedding in  $W$ <sup>+</sup> space (see also Fig. 8).

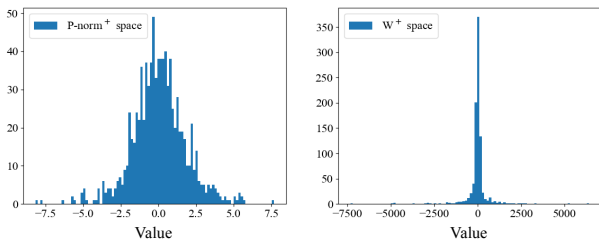


Figure 8: Histograms of the values of last 50 dimensions of the  $P$ -norm<sup>+</sup> and  $W$ <sup>+</sup> space embedding. Notice the range of values on the x-axis. The  $W$ <sup>+</sup> space embedding has a higher number of outliers which indicates overfitting.

#### 4.7. Histogram of the Embeddings

We analyze the quality of the embedding using the histograms in the  $P$ -norm<sup>+</sup> space. The embedding in this domain should follow a normal distribution with zero mean and unit variance in each dimension if the goal is to make embedded images similar to sampled ones. Here, we remark that the embedding quality is affected by two factors. First, the distribution of the approximately first 10 dimensions is critical in determining the editing quality. For example, in Fig. 6, we observe that some of the methods like PULSE and Encoders have a distribution that are more narrow. This indicates that the reconstruction quality is lower but the editing quality is higher. This can be observed in Table 1 and Table 2. Second, we observe that the embedding in  $P$ -norm<sup>+</sup> space (either projected from the  $W$ <sup>+</sup> space embedding or originally embedded in  $P$ -norm<sup>+</sup> space), tend to produce highly unstable values (outliers) in the later dimensions (See Fig. 7 and Fig. 8). We observe that a  $W$ <sup>+</sup>

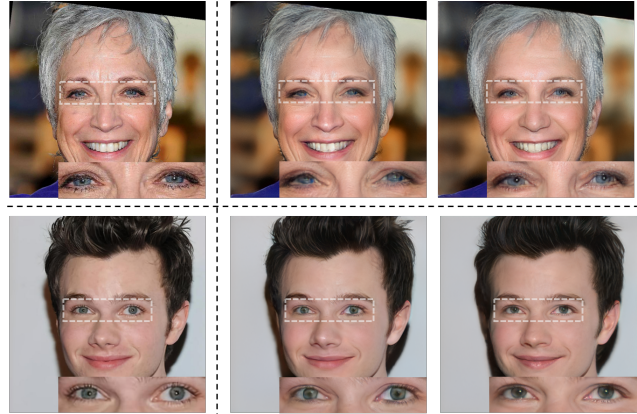


Figure 9: Eye correction obtained by applying the clipping regularizer in the  $P$ -norm<sup>+</sup> space on  $W$ <sup>+</sup> embedding. Left: original image, middle:  $W$ <sup>+</sup> embedding, right:  $W$ <sup>+</sup> embedding with  $P$ -norm<sup>+</sup> clipping regularizer.

space embedding has a higher number of such values as compared to the  $P$ -norm space embedding. Moreover, in Fig. 7 we observe that the latents move away from the mean face during the optimization (the mean face is the origin of  $P$ -norm space and it is computed by sampling 1M latents). This indicates that using a small number of iterations or adding a regularizer on the distance is a promising idea to prevent overfitting.

## 5. How to Derive IIS?

### 5.1. Improved Perceptual Regularizer

One important aspect of Image2StyleGAN is to use a perceptual regularizer. The original version suggested to use the VGG-perceptual loss [23]. However, we noticed that switching VGG to LPIPS [28] results in a noticeable improvement. Another detail of perceptual losses is that the publicly available networks mainly work for a smaller resolution, e.g.  $256 \times 256$ . Therefore, the generated image as well as the reference image need to be downsampled to evaluate the perceptual loss. Following PULSE [17] we also propose to use bicubic downsampling to compute the perceptual loss, rather than bilinear or nearest neighbor downsampling. Finally, for downsampling the reference image we propose to use Lanczos downsampling [26].

### 5.2. Picking the Right Space for the Embedding

To optimize a latent code, one can choose to optimize the variables describing a latent code in different spaces. The main choices we investigated were  $P$ -norm<sup>+</sup> space and  $W$ <sup>+</sup> space. The choice of space influences the behavior of the optimization. For example, using  $P$ -norm<sup>+</sup> space provides more protection from overfitting and the distribution of variables has fewer outliers. By contrast, optimizing in

$W^+$  space produces more outliers. See Fig. 8 for a visualization. This manifests itself in overfitting artifacts visible in teeth and eyes as described in the previous section. On the other hand, optimization in  $W^+$  space progresses faster and needs fewer steps than optimizing in  $P\text{-norm}^+$  space. We choose to optimize in  $W^+$  space, but apply the regularizer in  $P\text{-norm}^+$  space.

### 5.3. Distance Regularizer

Based on our results, it seems most promising to devise a regularizer that penalizes an embedding if it goes too far from the center. To this effect, there seem to be three simple strategies to evaluate for regularizing a latent code in  $P\text{-norm}^+$  space: 1) regularize the  $L_2$  distance from the center, possibly using separate weights along each dimension. 2) clipping values that are over a given threshold, possibly using a separate threshold per dimension. 3) projecting to a sphere / ellipsoid in a suitable space.

We propose to use a clipping based regularizer for our main method evaluated in this paper. We show additional ablation studies of the regularization in the supplementary material.

We propose to use a clipping regularizer that clips to the maximum values at each iteration (See Table 5). We apply a  $P\text{-norm}^+$  clipping regularizer (clipping larger values to  $2\sigma$  and  $-2\sigma$ ) to the embeddings in the  $P\text{-norm}^+$  as well as the  $W^+$  space and show improved results in terms of editing quality and realism (See Fig. 9) with a same or slight drop in the reconstruction quality. In Table 5, we compare results before and after the clipping regularizer. This also confirms that the statistics in  $P\text{-norm}^+$  space play an important role in finding where the good latents are and at the same time explain the reconstruction-editing quality trade-off. Finally, we also found a related paper on arXiv that presents similar ideas to our work [27].

## 6. Implementation Details

We collected a dataset of 100 images. 25% of this dataset are “in the wild” images and 75% of the images are derived from the CelebA HQ dataset [13]. For the regularization task (see Table 5), we selected a subset of 10 representative images which capture both diversity as well as the difficulty to embed (e.g. people with prominent wrinkles, people with hats, different eye gaze directions and mouth shapes etc). For our method, we used a learning rate of 0.01 with 1200 steps for all images. We used the ADAM optimizer with standard settings to obtain the results.

## 7. Limitations and Future Work

Our work has some limitations that we leave to future work. One limitation is that we did not investigate the joint distribution of the (18) different components of an extended

latent space and how the difference and similarity between components influences the embedding. From pure sampling, we know that sampling the 18 components randomly leads to poor results. However, it is unclear how similar they actually need to be, as we could not really observe a consistent difference when experimenting with different regularizers. In the future, we would like to investigate different regularizers that have been proposed to that effect (e.g. hierarchical optimization or an  $L_2$  similarity term) and propose our own.

## 8. Conclusion

We introduced the  $P\text{-norm}$  space as a tool to facilitate improved StyleGAN embedding and to analyze different embedding algorithms. We proposed a framework to compare the different aspects of different embedding algorithms and we discuss their strength and weaknesses. Finally, we proposed a novel StyleGAN embedding algorithm that provides the most desirable trade-off among all competing methods.

## References

- [1] Rameen Abdal, Yipeng Qin, and Peter Wonka. Image2stylegan: How to embed images into the stylegan latent space? In *Proceedings of the IEEE international conference on computer vision*, pages 4432–4441, 2019. 1, 2, 3, 5, 7, 8
- [2] Rameen Abdal, Yipeng Qin, and Peter Wonka. Image2stylegan++: How to edit the embedded images? In *Proceedings of the IEEE/CVF Conference on Computer Vision and Pattern Recognition*, pages 8296–8305, 2020. 2, 6
- [3] Rameen Abdal, Peihao Zhu, Niloy Mitra, and Peter Wonka. Styleflow: Attribute-conditioned exploration of stylegan-generated images using conditional continuous normalizing flows. *arXiv e-prints*, pages arXiv–2008, 2020. 6, 11
- [4] Martin Arjovsky, Soumith Chintala, and Léon Bottou. Wasserstein gan. *arXiv preprint arXiv:1701.07875*, 2017. 2
- [5] David Bau, Hendrik Strobelt, William Peebles, Bolei Zhou, Jun-Yan Zhu, Antonio Torralba, et al. Semantic photo manipulation with a generative image prior. *arXiv preprint arXiv:2005.07727*, 2020. 2
- [6] David Bau, Jun-Yan Zhu, Jonas Wulff, William Peebles, Hendrik Strobelt, Bolei Zhou, and Antonio Torralba. Seeing what a gan cannot generate. In *Proceedings of the IEEE International Conference on Computer Vision*, pages 4502–4511, 2019. 2
- [7] Anselm Blumer, Andrzej Ehrenfeucht, David Haussler, and Manfred K Warmuth. Occam’s razor. *Information processing letters*, 24(6):377–380, 1987. 2
- [8] Ian Goodfellow, Jean Pouget-Abadie, Mehdi Mirza, Bing Xu, David Warde-Farley, Sherjil Ozair, Aaron Courville, and Yoshua Bengio. Generative adversarial nets. In *Advances in neural information processing systems*, pages 2672–2680, 2014. 2

- [9] Jinjin Gu, Yujun Shen, and Bolei Zhou. Image processing using multi-code gan prior. In *Proceedings of the IEEE/CVF Conference on Computer Vision and Pattern Recognition*, pages 3012–3021, 2020. 6
- [10] Shanyan Guan, Ying Tai, Bingbing Ni, Feida Zhu, Feiyue Huang, and Xiaokang Yang. Collaborative learning for faster stylegan embedding. *arXiv preprint arXiv:2007.01758*, 2020. 2
- [11] Erik Härkönen, Aaron Hertzmann, Jaakko Lehtinen, and Sylvain Paris. Ganspace: Discovering interpretable gan controls. *arXiv preprint arXiv:2004.02546*, 2020. 6
- [12] Martin Heusel, Hubert Ramsauer, Thomas Unterthiner, Bernhard Nessler, and Sepp Hochreiter. Gans trained by a two time-scale update rule converge to a local nash equilibrium. In *Advances in neural information processing systems*, pages 6626–6637, 2017. 6
- [13] Tero Karras, Timo Aila, Samuli Laine, and Jaakko Lehtinen. Progressive growing of gans for improved quality, stability, and variation. *arXiv preprint arXiv:1710.10196*, 2017. 2, 9
- [14] Tero Karras, Miika Aittala, Janne Hellsten, Samuli Laine, Jaakko Lehtinen, and Timo Aila. Training generative adversarial networks with limited data. In *Proc. NeurIPS*, 2020. 1, 2
- [15] Tero Karras, Samuli Laine, and Timo Aila. A style-based generator architecture for generative adversarial networks. In *Proceedings of the IEEE conference on computer vision and pattern recognition*, pages 4401–4410, 2019. 1, 2, 6, 7, 8
- [16] Tero Karras, Samuli Laine, Miika Aittala, Janne Hellsten, Jaakko Lehtinen, and Timo Aila. Analyzing and improving the image quality of stylegan. In *Proceedings of the IEEE/CVF Conference on Computer Vision and Pattern Recognition*, pages 8110–8119, 2020. 1, 2, 3, 5
- [17] Sachit Menon, Alexandru Damian, Shijia Hu, Nikhil Ravi, and Cynthia Rudin. Pulse: Self-supervised photo upsampling via latent space exploration of generative models. In *Proceedings of the IEEE/CVF Conference on Computer Vision and Pattern Recognition*, pages 2437–2445, 2020. 1, 2, 3, 5, 8
- [18] Microsoft. Azure face, 2020. 6
- [19] Takeru Miyato, Toshiki Kataoka, Masanori Koyama, and Yuichi Yoshida. Spectral normalization for generative adversarial networks. *arXiv preprint arXiv:1802.05957*, 2018. 2
- [20] Alec Radford, Luke Metz, and Soumith Chintala. Unsupervised representation learning with deep convolutional generative adversarial networks. *arXiv preprint arXiv:1511.06434*, 2015. 2
- [21] robertluxemburg. Github repository: stylegan2encoder. <https://github.com/robertluxemburg/stylegan2encoder>, 2020. 1, 3, 5
- [22] Yujun Shen, Ceyuan Yang, Xiaoou Tang, and Bolei Zhou. Interfacegan: Interpreting the disentangled face representation learned by gans. *arXiv preprint arXiv:2005.09635*, 2020. 6
- [23] Karen Simonyan and Andrew Zisserman. Very deep convolutional networks for large-scale image recognition. *arXiv preprint arXiv:1409.1556*, 2014. 3, 8
- [24] Ayush Tewari, Mohamed Elgharib, Florian Bernard, Hans-Peter Seidel, Patrick Pérez, Michael Zollhöfer, Christian Theobalt, et al. Pie: Portrait image embedding for semantic control. *arXiv preprint arXiv:2009.09485*, 2020. 2, 7
- [25] Ayush Tewari, Mohamed Elgharib, Gaurav Bharaj, Florian Bernard, Hans-Peter Seidel, Patrick Pérez, Michael Zollhofer, and Christian Theobalt. Stylerig: Rigging stylegan for 3d control over portrait images. In *Proceedings of the IEEE/CVF Conference on Computer Vision and Pattern Recognition*, pages 6142–6151, 2020. 6
- [26] Ken Turkowski. Turkowski filters for common resampling tasks 10 april 1990 filters for common resampling tasks. 8
- [27] Jonas Wulff and Antonio Torralba. Improving inversion and generation diversity in stylegan using a gaussianized latent space, 2020. 9
- [28] Richard Zhang, Phillip Isola, Alexei A Efros, Eli Shechtman, and Oliver Wang. The unreasonable effectiveness of deep features as a perceptual metric. In *CVPR*, 2018. 3, 8
- [29] Jiapeng Zhu, Yujun Shen, Deli Zhao, and Bolei Zhou. In-domain gan inversion for real image editing. In *Proceedings of European Conference on Computer Vision (ECCV)*, 2020. 2, 6, 7
- [30] Jun-Yan Zhu, Philipp Krähenbühl, Eli Shechtman, and Alexei A Efros. Generative visual manipulation on the natural image manifold. In *European conference on computer vision*, pages 597–613. Springer, 2016. 2

## A. Ablation Study of Regularizers

In this section, we discuss the effect of the regularizers on the editing quality and the realism of the embedded images with a small drop in reconstruction quality. Here, we regularize in the proposed  $P\text{-norm}^+$  space. We show three types of regularizers in Table 6 and Table 7.

- The first one is the clipping regularizer, where we clip the values in the  $P\text{-norm}^+$  space based on some threshold.
- The second method is the spherical projection where each dimension in the  $P\text{-norm}^+$  is re-projected to a hyper-sphere of a given radius. Note that here we consider that each dimension in  $P\text{-norm}^+$  as a 18 dimensional vector due to the 18 layers. we calculate the norm for each  $P\text{-norm}^+$  dimension and compare it with the given radius for reprojection.
- The third method considers the L2-norm squared for each layer in  $P\text{-norm}^+$  space. Note that since its added to the loss term, the ablation study of the weight given to this term is mentioned.

We also ablate the learning rate and the number of optimization steps in Table 6 and Table 7. We notice that the embedding quality is very sensitive to these parameters. For example, even though the reconstruction quality is better with learning rate 0.1 with the number of steps equal to 1k, the editing quality metrics suffer especially in the  $W^+$  space projection. Hence, we recommend to use a lower learning rate with an increased number of steps as that always converges to a good solution that has both good reconstruction as well as good editing quality. Based on the Table 6, Table 7 and Fig. 14, for the Clipping method, we observe that the good reconstruction range is from clip 2 – 10 and the good editing range is from clip 1 – 7. Hence we recommend that the optimal range for a better trade-off is between 2 – 7 in this case. In Spherical projection method, we observe that the good reconstruction range is from clip 5 – 10 and the good editing range is from clip 1 – 5. Hence we recommend that a better trade-off is achieved at 5. Similarly, in case of the L2-norm squared regularizer, the two ranges for the weights are  $1e-8$  to  $1e-7$  and  $1e-7$  to  $1e-5$  respectively. Hence we select  $1e-7$  in this case. All these settings provide better trade-offs for the reconstruction quality - editing quality of the embeddings.

## B. Realism and editing

In this section we discuss the visual comparisons of the reconstruction quality, realism and the editing quality of our method with other competing methods. Fig 10 and Fig. 11 shows the comparison of the reconstruction quality and realism of our method using the clipping regularizer versus

other methods. Note that our method preserves the realism in an image with better eye and teeth embeddings. Moreover, in Fig. 12, we show the comparison of style mixing results achieved by different methods. Note that our method better preserves the shape of the original content image and only the styles are transferred. In Fig 13, we show the  $W^+$  and  $P\text{-norm}^+$  interpolation results. In  $P\text{-norm}^+$  interpolation, we project the  $W^+$  codes into the  $P\text{-norm}^+$  space and vice versa. The degradation of the interpolation quality of  $W^+$  embedding projected into  $P\text{-norm}^+$  space indicates that the embeddings do not represent a better reconstruction quality - editing quality trade-off and hence the editing quality suffers.

## C. Edits with StyleFlow

We also show the edits achieved by the StyleFlow [3] method on our embeddings in the supplementary video [https://youtu.be/3x\\_mIn\\_QPpk](https://youtu.be/3x_mIn_QPpk). The results show that our embedding method is able to produce realistic results using StyleFlow compared to I2S\*. Note that our embedding produces better results when subjected to sequential edits. Here we perform different edits to the embedded image like lighting, gender change, expression change, adding glasses, pose changes, age and hair.

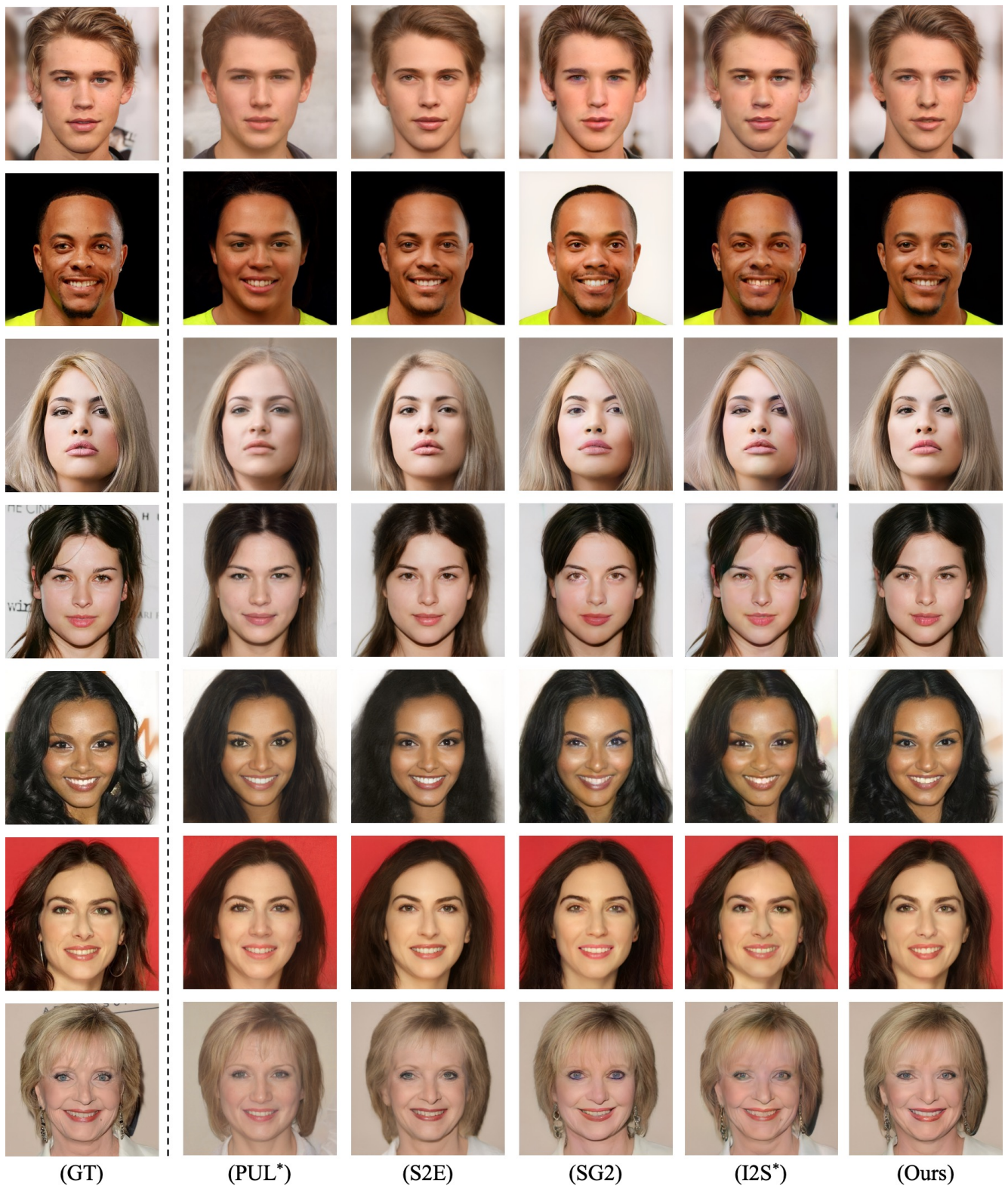


Figure 10: Figure showing the reconstruction quality results. Notice that our results are more realistic with better eye and teeth embeddings.

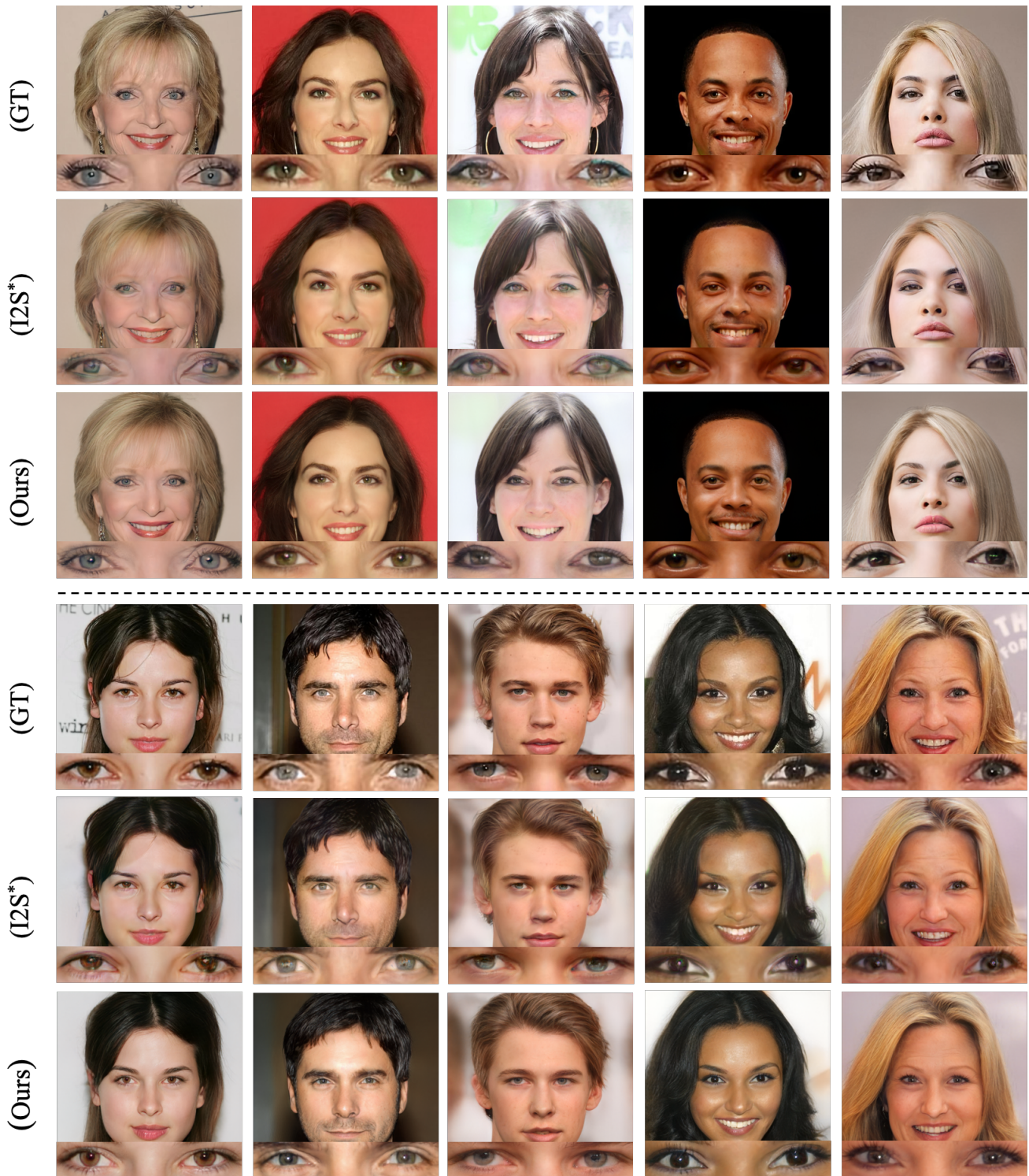


Figure 11: Zoomed-in results of reconstruction showing differences in eye embeddings.

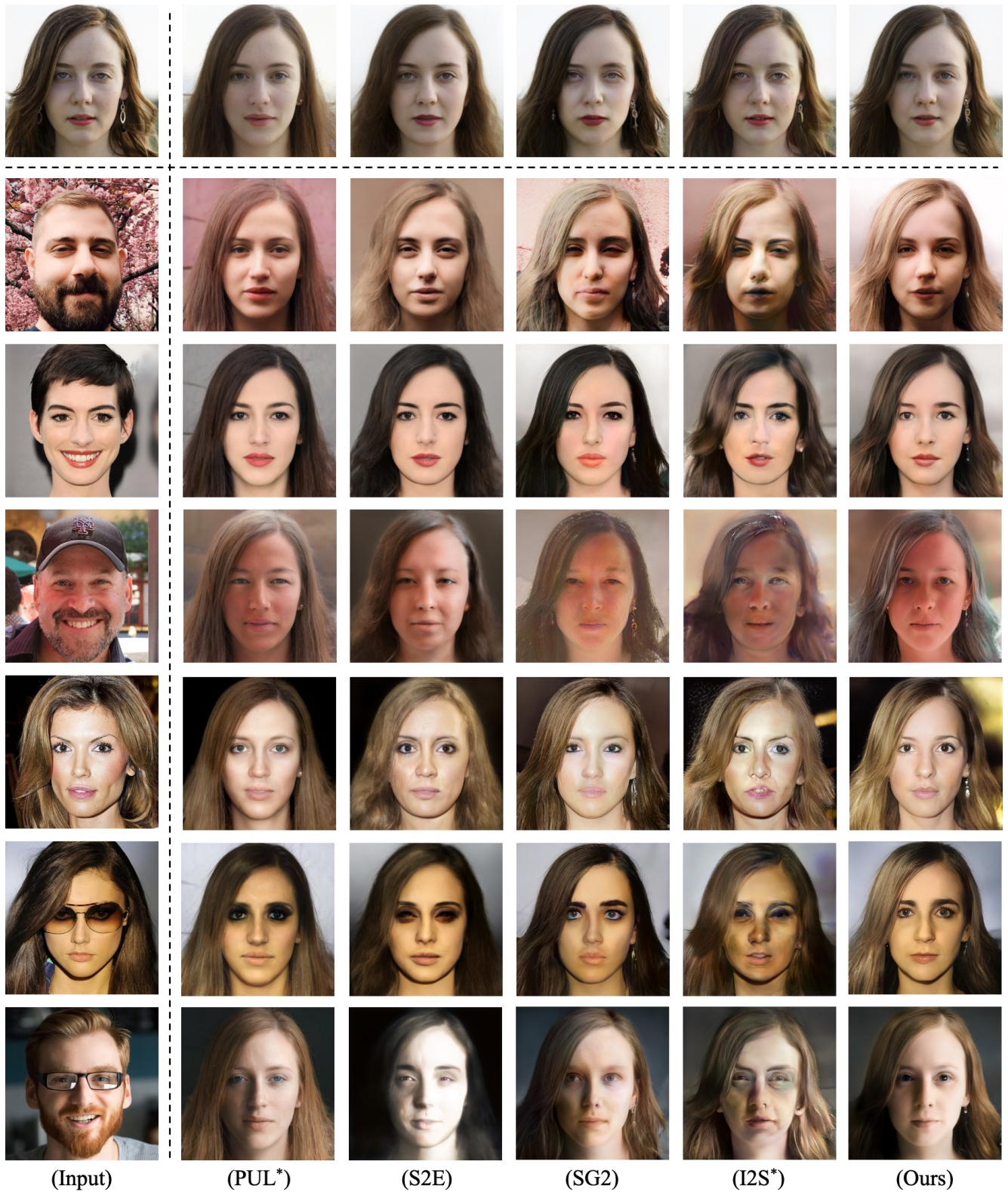


Figure 12: Style mixing comparison between different methods. The top row represents the embeddings of content image and the first column represents the style images. Note here we transfer the last 11 layers. Also note that our results tend to better retain the shape and has less artifacts.

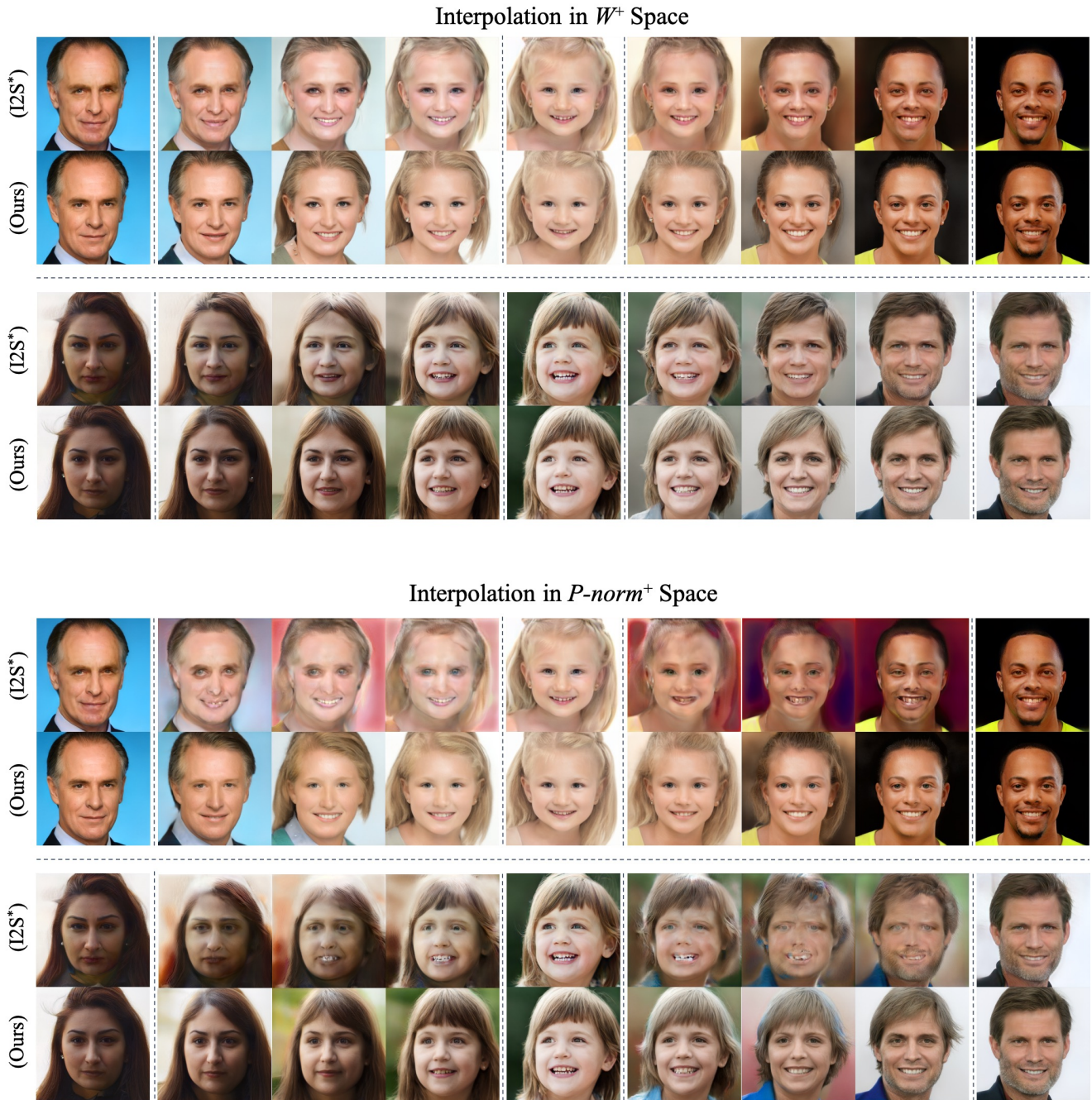


Figure 13: Interpolation results in the  $W^+$  ( $I2S^*$ ) space and  $P\text{-norm}^+$  space. In this figure, the first, the middle and the last columns represent the original embedded images. In "Interpolation in  $W^+$  Space", the first and third row represent  $I2S^*$  code interpolation and the second and fourth row represent interpolation of codes produced by our method projected in  $W^+$  space. In "Interpolation in  $P\text{-norm}^+$  Space", the first and third row represent  $I2S^*$  code interpolation projected in  $P\text{-norm}^+$  space and the second and fourth row represent interpolation of codes produced by our method.

lr	Regularizer	Reconstruction Metrics					StyleMix
		SSIM $\uparrow$	RMSE $\downarrow$	PSNR $\uparrow$	VGG $\downarrow$	LPIPS $\downarrow$	FID $\downarrow$
0.1		0.82	0.07	24.08	0.63	0.15	154.82
		0.83	0.06	24.43	0.61	0.14	136.79
	Clip-1	0.77	0.09	20.88	0.86	0.26	126.30
	<b>Clip-2</b>	0.79	0.07	22.53	0.76	0.21	124.87
	<b>Clip-5</b>	0.82	0.07	23.43	0.68	0.17	135.97
	<b>Clip-7</b>	0.82	0.07	23.77	0.67	0.17	138.14
	Clip-10	0.82	0.07	23.77	0.66	0.16	135.01
	Project-1	0.78	0.09	21.06	0.87	0.26	125.46
	Project-2	0.78	0.09	21.51	0.84	0.24	126.95
	0.01	<b>Project-5</b>	0.80	0.08	22.48	0.77	0.21
Project-7		0.81	0.07	22.87	0.73	0.20	136.35
Project-10		0.82	0.07	23.57	0.68	0.17	140.52
L2-1e-4		0.66	0.19	14.32	1.45	0.53	208.72
L2-1e-5		0.70	0.14	16.97	1.22	0.43	152.51
L2-1e-6		0.74	0.11	19.32	0.96	0.31	120.25
<b>L2-1e-7</b>		0.80	0.08	21.71	0.80	0.22	122.81
L2-1e-8		0.82	0.06	23.91	0.64	0.16	137.43

Table 6: Reconstruction Metrics and StyleMix using Clipping (Clip), Spherical projection (Project), and L2-norm squared regularizers. Note that the parameters are mentioned after the method *e.g.* Clip-1 refers to clipping regularizer with the range from  $-\sigma$  to  $\sigma$ , Project-1 refers to Spherical regularizer with radius 1, L2  $1e-4$  refers to L2-norm squared regularizer with weight  $1e-4$  in the loss term and so on. The choices marked as bold are the recommended settings.

lr	Regularizer	Pose Metrics					Interpolation Metrics	
		$-2\sigma \uparrow$	$-1\sigma \uparrow$	0	$1\sigma \downarrow$	$2\sigma \downarrow$	$W^+$ Space $\downarrow$	$P - norm^+$ Space $\downarrow$
0.1		6.75	3.96	0.80	-2.76	-4.98	129.44	266.72
		20.68	10.31	-0.56	-10.77	-20.44	116.33	223.34
	Clip-1	25.26	11.95	0.27	-11.99	-21.75	121.71	122.12
	<b>Clip-2</b>	23.13	12.15	-0.02	-12.42	-24.00	121.83	130.84
	<b>Clip-5</b>	23.55	10.87	-0.01	-11.06	-22.16	119.89	142.22
	<b>Clip-7</b>	22.61	11.28	-0.75	-12.29	-22.87	120.56	136.08
	Clip-10	22.94	11.74	-0.25	-11.31	-20.36	119.01	158.41
	Project-1	23.65	13.06	0.72	-10.36	-19.56	117.78	124.11
	Project-2	21.56	12.33	0.26	-12.75	-23.53	123.47	124.26
	0.01	<b>Project-5</b>	19.38	9.70	0.25	-8.62	-18.92	129.77
Project-7		19.31	9.22	-1.73	-10.82	-19.16	125.72	291.69
Project-10		20.74	10.99	0.32	-9.82	-17.69	121.58	372.70
L2-1e-4		22.08	10.60	-0.08	-9.25	-19.28	217.87	218.07
L2-1e-5		22.50	10.72	-0.47	-9.54	-18.96	161.67	161.35
L2-1e-6		27.69	13.21	-0.16	-12.92	-23.24	123.68	122.70
<b>L2-1e-7</b>		25.94	12.74	-0.38	-15.06	-25.91	118.23	118.44
L2-1e-8		21.48	11.08	-0.85	-12.76	-23.57	116.31	177.42

Table 7: Pose and Interpolation metrics using Clipping (Clip), Spherical projection (Project), and L2-norm squared regularizers. The choices marked as bold are the recommended settings.

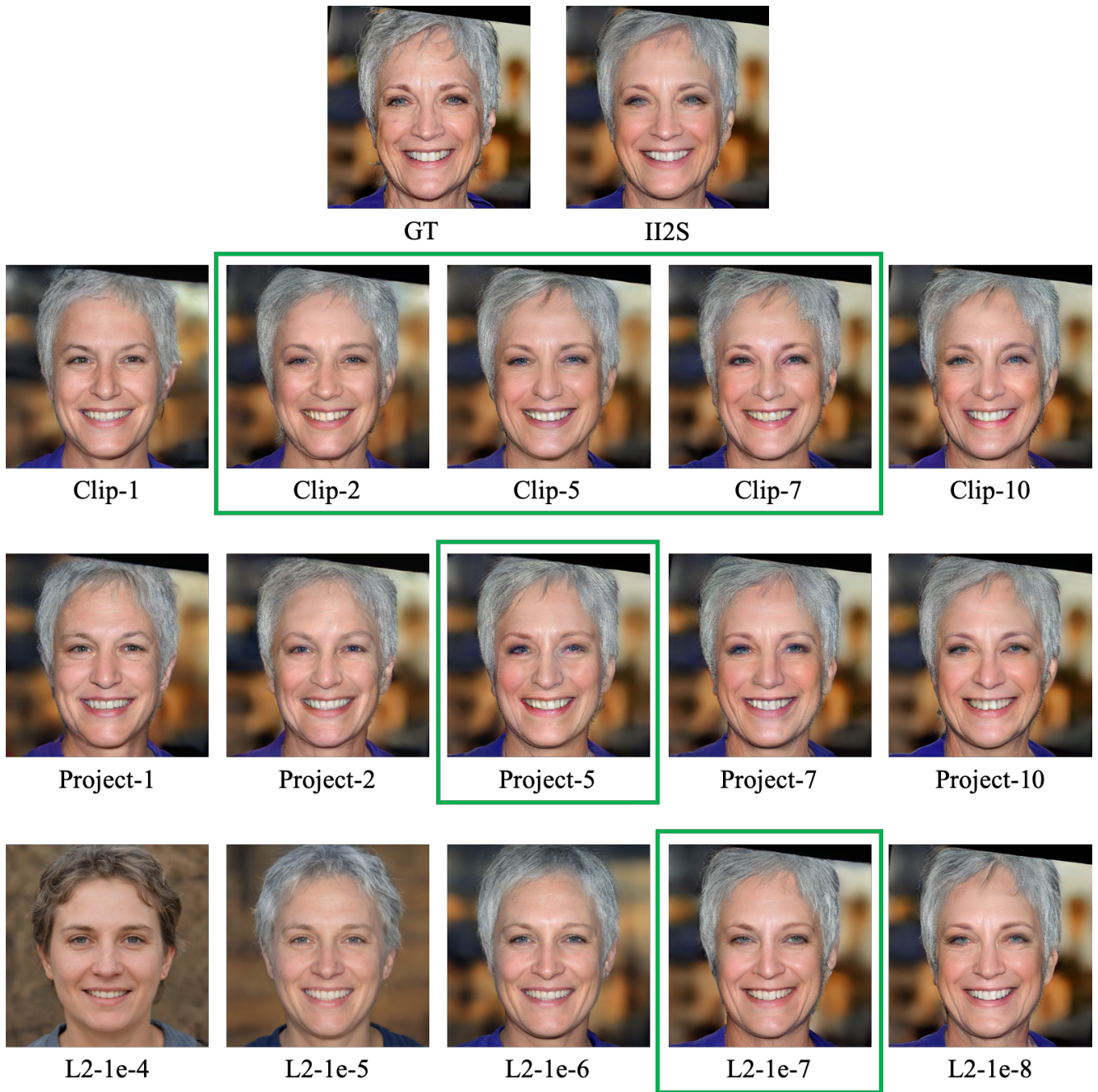


Figure 14: Figure showing the image embeddings using our I2S method with different regularizers.